LA-UR- 04-7334

Approved for public release;
distribution is unlimited.

Title: Modal Testing Variability of Spherical Marine Floats

Author(s): A. Robertson, F. Hemez, I. Salazar, and T. Duffey

Engineering Sciences and Applications Division
Weapon Response Group
Los Alamos National Laboratory
Los Alamos, NM 87545

Submitted to: IMAC XXIII

Rosen Plaza Hotel
Orlando , Florida USA
January 31 - February 3, 2005

Modal Testing Variability of Spherical Marine Floats

A. Robertson, F. Hemez, I. Salazar, and T. Duffey

Engineering Sciences and Applications Division
Weapon Response Group
Los Alamos National Laboratory
Los Alamos, NM 87545

ABSTRACT

This study investigates the variability in modal data obtained from testing a set of hollow, almost spherical marine floats. Four sources of variability are investigated: unit-to-unit variability, operator-to-operator variability, test repetition, and accelerometer placement. Because moving the accelerometers implies a test setup reconfiguration, it is expected that variability due to accelerometer placement should encompass variability due to test repetition. Similarly, the unit-to-unit variability should encompass both accelerometer placement variability and test-to-test variability. Impulse and frequency response functions are estimated from the measured excitation and response of the marine floats. A series of techniques are then used to assess the variation of the modal properties between each test, including: a measure of the spread of the frequency response functions in each test group; the variation of the temporal moments, spectral moments, and principal components; and the variability of resonant frequencies and modal damping ratios extracted from the data. The effects of mass and geometry on variability are also investigated. A strong correlation between the frequency and mass is found for the fundamental mode only. The main conclusion is that the majority of analysis techniques find the unit-to-unit variability to be the largest by a significant margin. The second largest is the variability caused by accelerometer placement. Next are the operator-to-operator variability and test-to-test variability.

INTRODUCTION

The main motivation for the study was to understand the natural variability when performing simple tests in a well-controlled environment. Understanding the variability and quantifying where it comes from is important for the development of numerical models that predict the structural response of spherical geometries. Although the analytical and numerical modeling of spheres has been extensively studied in the literature, little information is available on the degree of variability that can be expected from a lot of nominally identical, manufactured spheres. Clearly, such variability needs to be known to guide the level of accuracy of numerical models.

The objects used in the study were a set of nominally "identical", hollow, almost spherical marine floats. A previous study demonstrated that the population of marine floats exhibit significant geometric variability [1]. The first source of variability to consider is therefore the unit-to-unit variability (denoted by the symbol $\mathbf{U_2U}$). U_2U variability includes other sources of variability that may not be directly related to variations of the individual components tested. These are the test-to-test ($\mathbf{T_2T}$) and operator-to-operator ($\mathbf{O_2O}$) sources of variability. T_2T refers to the variability obtained when the same modal test is repeated in the same conditions with the same marine float. Responsible for T_2T variability might be small changes in the operating conditions (the location of impact is not always exactly the same), environmental conditions (such as temperature changes), etc. Another possible cause of T_2T variability is the placement of the accelerometers on the part. We will consider this variability separately and will label it as **Acc**. O_2O refers to the variability obtained when two different people perform the same modal test and data analysis. The breakdown of sources of variability into T_2T, Acc, U_2U and O_2O is not meant to be exhaustive.

Force and acceleration responses were obtained from the modal testing of the floats. From this data, the analysis was two-fold. First was the identification of the system's dynamic properties and, second, the statistical analysis of the identification results. From the time series, the frequency response functions of the system were estimated and modal parameters (resonant frequencies, mode shapes and modal damping ratios) identified. The second step was to analyze the statistical variations obtained and attempt to explain them through correlation with various factors that control the characteristics of the population tested. The variation in the modal properties of the floats was assessed in a variety of ways, including modal frequencies and features extracted from the modal response data.

EXPERIMENTAL MODAL ANALYSIS

Test Configuration

The test components are "off-the-shelf," commercially available marine floats (see Figure 1) commonly used by the petrochemical industries in large open or closed tanks for liquid level (gage) measurements [1,2,3]. The marine floats were purchased directly from Quality Float Works in Schaumburg, Illinois [3]. Each float has a 9-inch outside diameter, 16-gage shell thickness, and no optional external piping connections. They are made from Type 304L stainless steel in two hemispheres that are welded together. The float also has a weld at the top, sealing it from outside air.

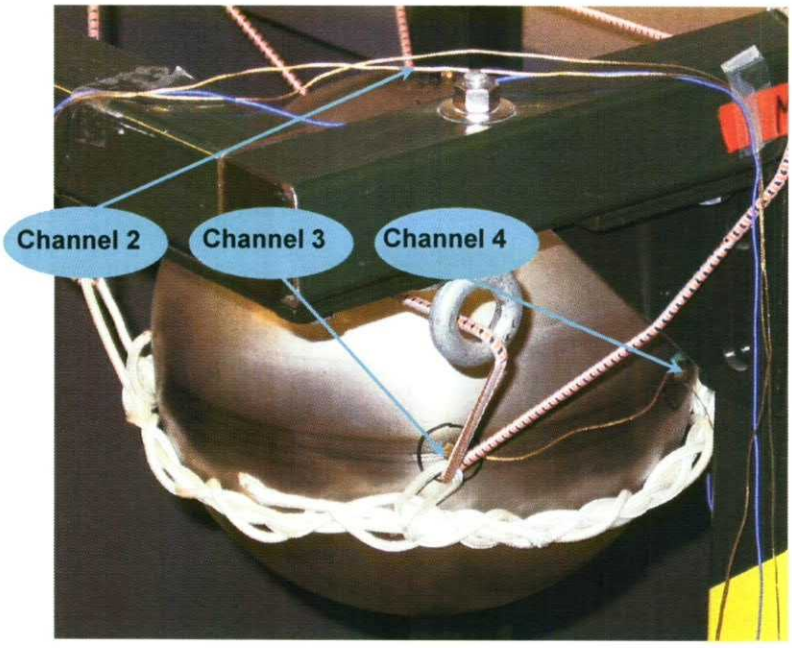

Figure 1: Marine float hanging in test apparatus with accelerometers

The apparatus used for the modal testing of the floats consisted of a braided rope ring supported by four points on a three-legged frame with elastic cord, as shown Figure 1. We placed each float into the rope ring with the equatorial weld horizontal and the polar weld facing up. We used three accelerometers to measure the modal response: two accelerometers were placed sixty degrees apart on the equator (Channels 3 and 4), and a third accelerometer was placed on the pole beside the weld (Channel 2).

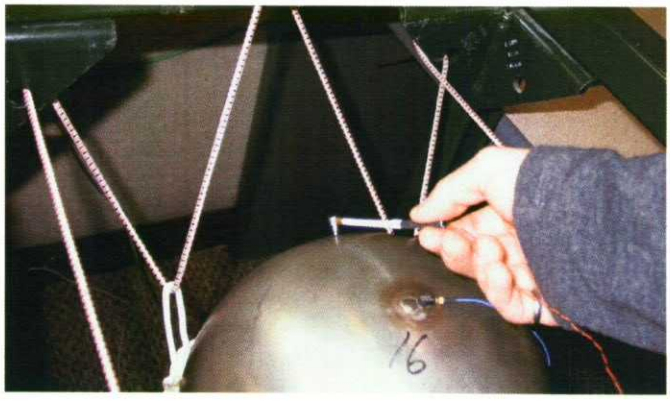

Figure 2: Impact location

Experimental Procedure

We used a small impact hammer to excite the high-frequency modes of the float. We marked the excitation point on the float at forty-five degrees from the polar axis away from the accelerometers placed on the equator weld. Figure 2 shows the excitation point being impacted with the impact hammer.

We recorded a measurement of both the input force and the output acceleration at the three accelerometer locations for each test. The sampling frequency was 20,480 Hz, with a data-block size of 4,096. We used a Dactron data-acquisition system, which performs antialiasing on the data and averaging in the frequency domain. The number of averages for each data set was equal to ten. Table 1 summarizes the tests performed, which are then described in detail below.

Table 1: Summary of the modal tests performed.

Type of Test	Number of Replicates	Number of Averages	Bandwidth	Number of the Float Used
U_2U	14	10	0-10.24 kHz	11,12,14-20,23,25,27-29
T_2T	10	10	0-10.24 kHz	16
Acc	10	10	0-10.24 kHz	16
O_2O	4	10	0-10.24 kHz	16

Unit-to-Unit (U_2U) Variability

We carefully tested the population of fourteen floats using the same procedure to quantify the U_2U variability. Each of the fourteen floats was instrumented with accelerometers and placed in the rope ring for testing. Each U_2U variability data set consists of fourteen replicates, one for each float, and each replicate consists of ten averaged runs. Once we obtained data for all fourteen floats, we chose a nominal float (number 16), and conducted three sets of tests: the T_2T variability test, Acc variability test, and O_2O variability test.

Test-to-Test (T_2T) Variability

For the T_2T test, the float was removed from the wire rope suspension system and carefully replaced with the equatorial weld oriented as close to horizontal as possible. Each T_2T variability data set consists of ten replicates with each replicate consisting of ten averaged runs.

Accelerometer (Acc) Variability

Next, we examined the sensitivity of accelerometer placement on the equatorial weld. The accelerometers were slightly misplaced and the test was repeated. Because the float needed to be removed from the rope ring, variability obtained from the suspension system placement was included in the Acc variability test. We used the first eight tests to change the two accelerometers placed on the equator, and the last two tests examined the effect of the placement of the accelerometer on the pole.

Operator-to-Operator (O_2O) Variability

Finally, we considered O_2O variability by repeating the same test with four different operators. Each O_2O variability data set consists of four replicates with each replicate consisting of ten averaged runs. We left the float in the same position for each O_2O test, and the accelerometers remained in the same configuration.

RESULTS

From each of the modal tests performed, impulse response functions (IRFs) and frequency response functions (FRFs) were calculated from the input/output data. Upon examination of the data, it was found that accelerometer 2 had the cleanest response signal, so it was decided to only use this channel for analysis. Note that since only the last two of the ten Acc tests involved moving accelerometer 2, only the last three Acc tests will be used for analysis. The IRFs and FRFs from accelerometer 2 were analyzed to assess the amount of variation present in the data caused by the different testing groups presented above: U_2U, T_2T, Acc, and O_2O. A variety of methods were used to assess this variability, and the results are summarized in this section.

Frequency Response Data

To assess the level of variability in each of the test groups, the envelope of the FRFs for each group was compared to the overall envelope of all of the test data. The analysis was restricted to the region of the frequency spectrum that contained the first few modes, specifically between 5000 and 6800 Hz. The envelopes were calculated by taking the minimum and maximum values of the FRF at each frequency value. Figure 3 shows that the U_2U variability accounts for most of the variability in the test data. It is difficult to discern from this figure which of the remaining variability sources has the next largest envelope. The standard deviation of the FRFs within each test group was taken to assess which had the largest variability. These values are shown in Figure 4 and provide an easy to interpret summary of which group contributed the most to the overall variability of the FRF data.

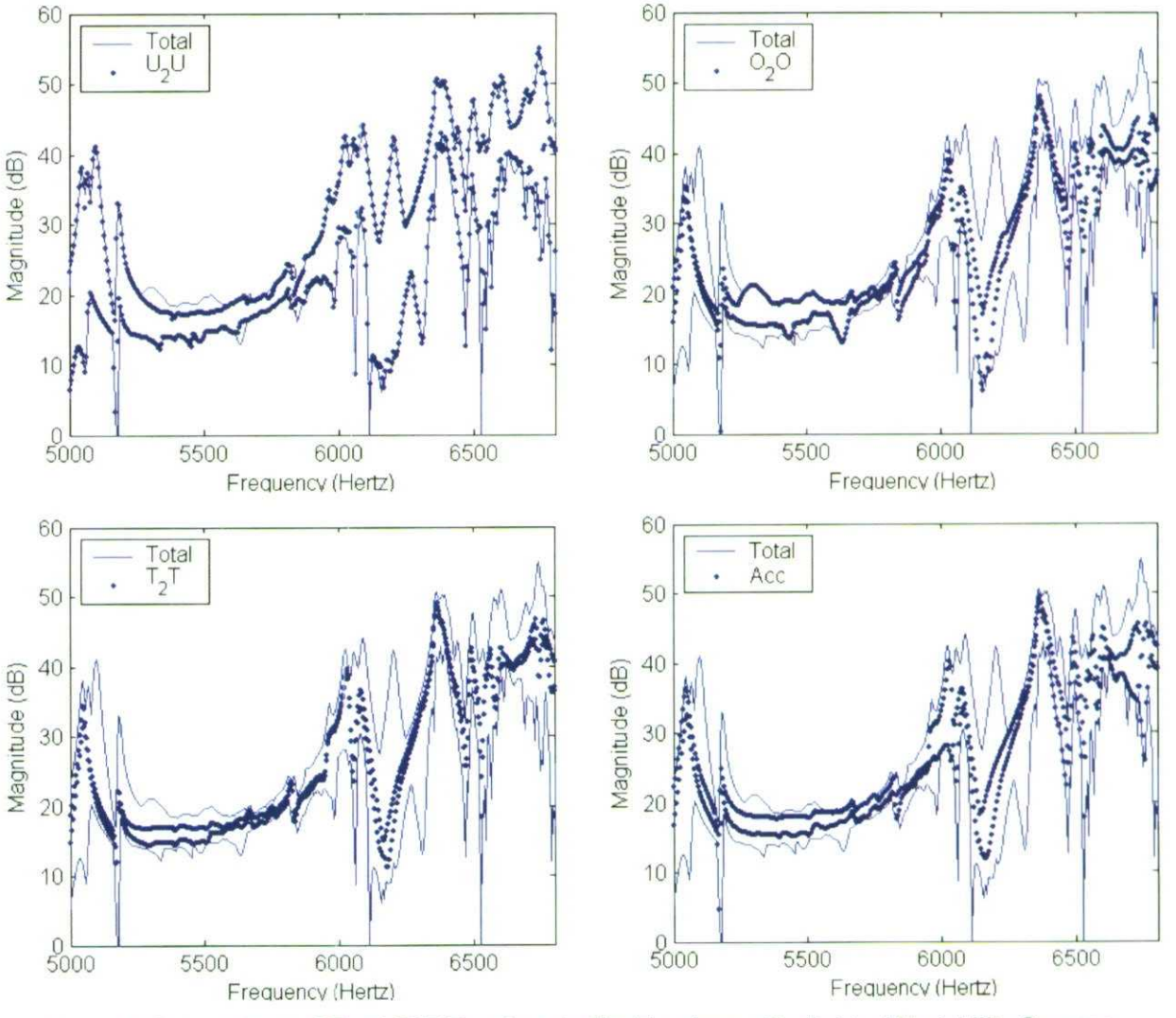

Figure 3: Comparison of Total FRF Envelope to the Envelope of Individual Variability Sources

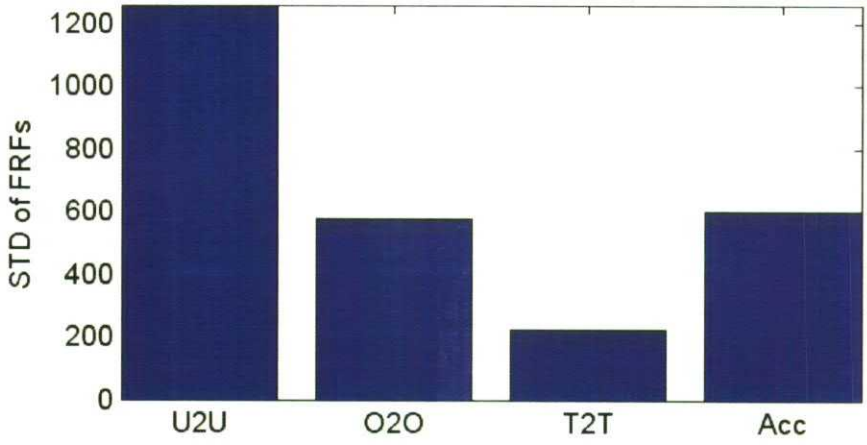

Figure 4: Standard deviation of the FRFs within each test group

ERA Fit

ERA is an eigensystem realization algorithm [4] that converts time-domain data to modal frequencies, modal damping ratios, and mode shapes. We used the ERA fit to determine the spread of modal frequencies obtained for all tests. We restricted our analysis to the first four modes of the system; Figure 5 shows the results, with frequency on the horizontal axis, damping on the vertical axis, and various symbols representing the results from all data sets collected.

Figure 6 displays the standard deviation for each of the four modes shown in the above plots. As expected, the standard deviations of the U_2U and Acc tests are in general higher than the standard deviations of the other tests. However, Acc variability is higher than U_2U variability for mode 4, which contradicts the assumption that U_2U variability should encompass Acc variability. Also, T_2T variability is larger than Acc for the first mode, which also contradicts the assumption that Acc variability should encompass T_2T variability.

Mass Correlation

One of the contributing factors to the modal frequencies of a sphere is its mass. In this case, the nominally identical floats have slightly different masses, with two distinct groupings. We therefore were interested to determine if the mass was a large factor in the variability of the identified frequencies. The sample of floats examined for the U_2U tests included five floats from the lower mass group and nine floats from the higher mass group. The mass correlation is illustrated in Figure 7. This plot of float mass versus identified frequency reveals that the frequency values for the lower-mass floats have more variability than those for the higher-mass floats. For the first mode, the amount of variability in the frequency measurements is smaller, and we observed a clear relationship between float mass and modal frequency. The relationship is negative, as it should be, because an increase in mass decreases the modal frequency value.

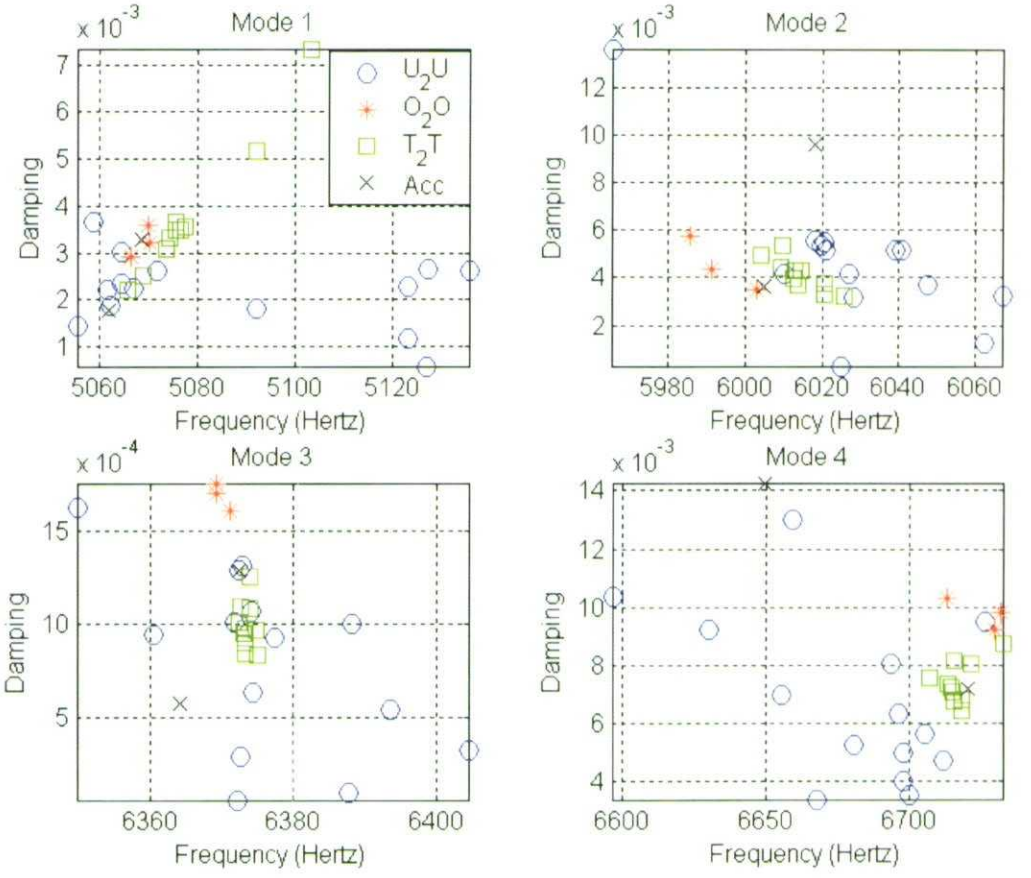

Figure 5: ERA-fit results showing frequency and damping variability for the first four modes

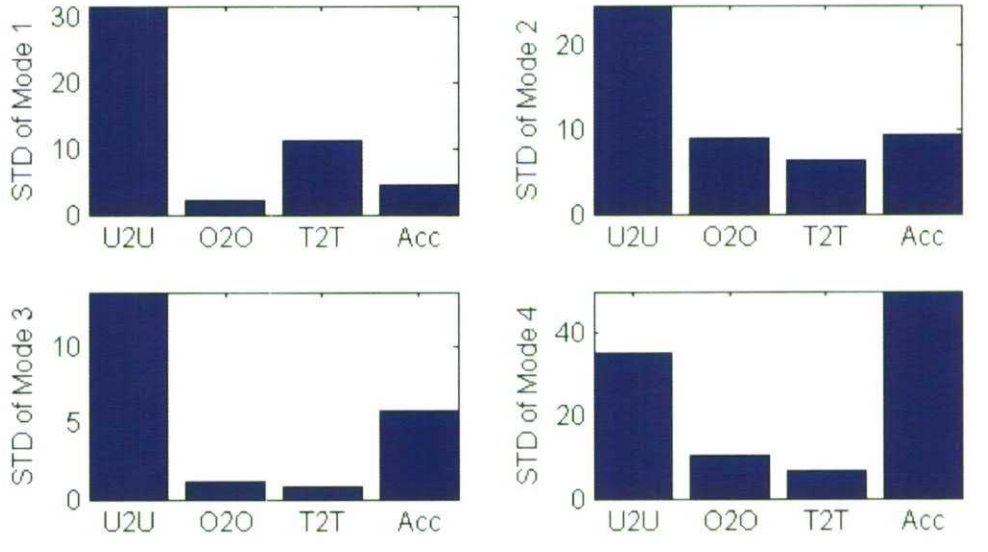

Figure 6: ERA-fit results: standard deviation of the first four modes across replicate tests

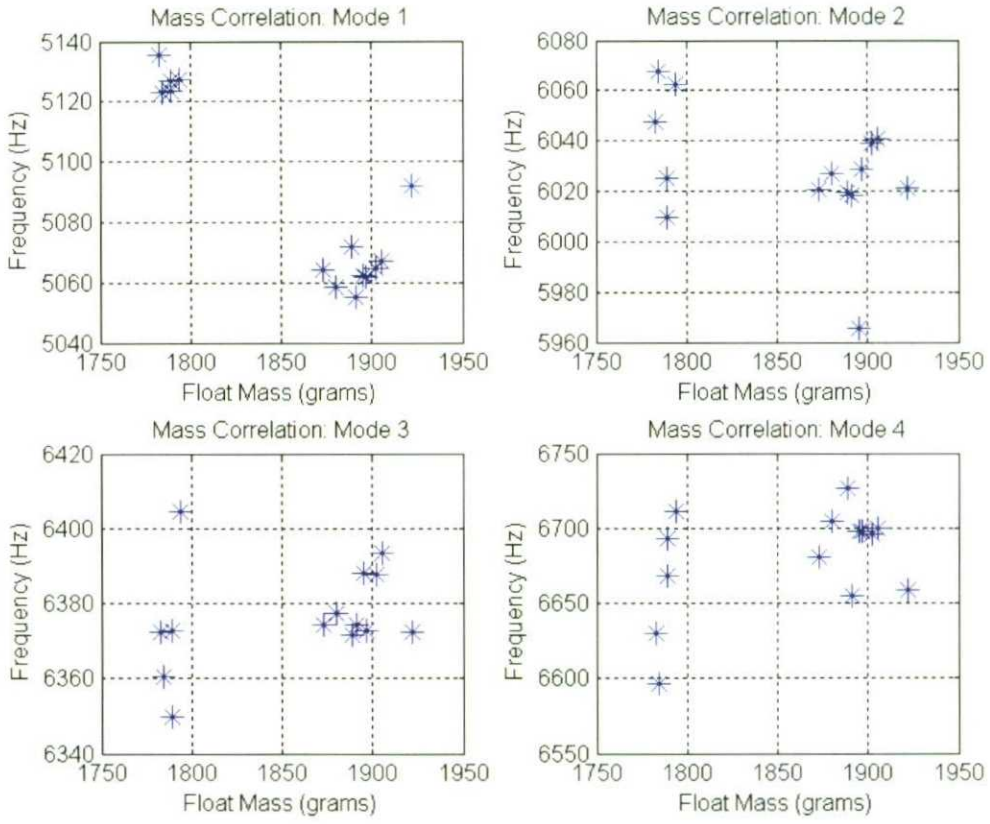

Figure 7: Mass correlation for the first four modes

Feature Extraction for Variability Assessment

Normally, when trying to assess the variability (uncertainty) in a set of test data, we do not look at the FRFs or even the modal frequencies themselves, due to their high dimensionality. Instead, we extract features from the data that we believe represent the important dynamics of the system. Feature extraction is the mapping of a data vector into a lower-dimensional feature vector. This mapping can be achieved by a linear or nonlinear transformation, the transformation chosen so as to retain as much relevant information as possible. This allows for an easier comparison between data sets. These features may also be more meaningful than the raw data, therefore enhancing the interpretability of the data. In these next two sub-sections we will be looking at some common features used to compare the results from multiple tests, and see how they vary for the given groups of tests performed.

Temporal and Spectral Moments

Temporal moments are a measure of the time statistics of a signal. They are used here to find another means for estimating the variability in the data. We focused on only the first three temporal moments, which are [5]:

- E = Energy, [g^2].
- *Tau* or T = Delay to the centroid of data, [sec].
- D = Central normalized RMS duration, [sec].

The features E, T, and D are calculated as follows:

$$E = \sum_{0 \le t \le N} x(t)^2 \tag{1}$$

$$T = \frac{1}{E} \sum_{0 \le t \le N} t \cdot x(t)^2 \tag{2}$$

$$D^2 = \frac{1}{E} \sum_{0 \le t \le N} t^2 \cdot x(t)^2 - T^2 \tag{3}$$

where *x(t)* is the impulse-response-time history for this analysis. We extracted the three temporal moments for each impulse-response measurement on Channel 2. Then, we assessed the standard deviation of these indicators inside each test group. As shown in Figure 8, the relative levels of variation between test groups are almost the same for each of the three temporal moments. U_2U variation far outweighs the effects of a different operator (O_2O), test setup (T_2T), or Acc.

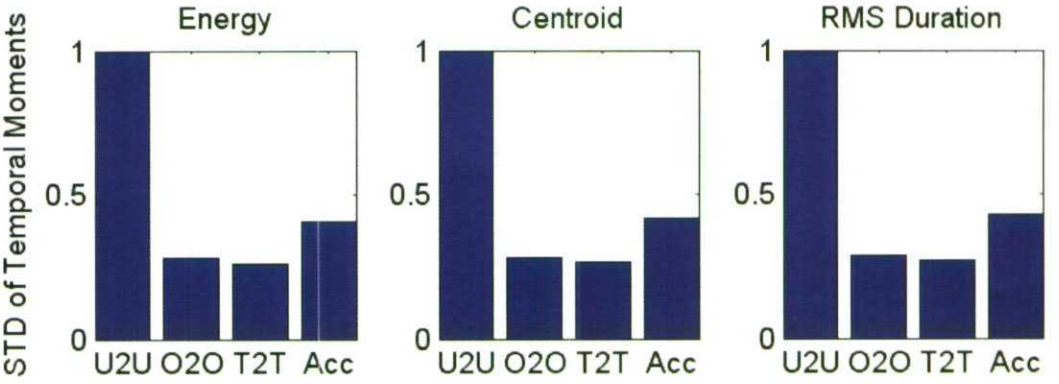

Figure 8: Normalized standard deviation of *E*, *Tau*, and *D* for impulse responses from Channel 2.

By substituting frequency for time in equations 1–3, we find the spectral moments of the response data. The interpretation is the same, with energy being the energy in the frequency domain, and similarly for the centroid and RMS duration. Figure 9 gives the normalized standard deviation of the spectral moments for the frequency-response function from Channel 2 for each test group. The results are very similar to the temporal moments.

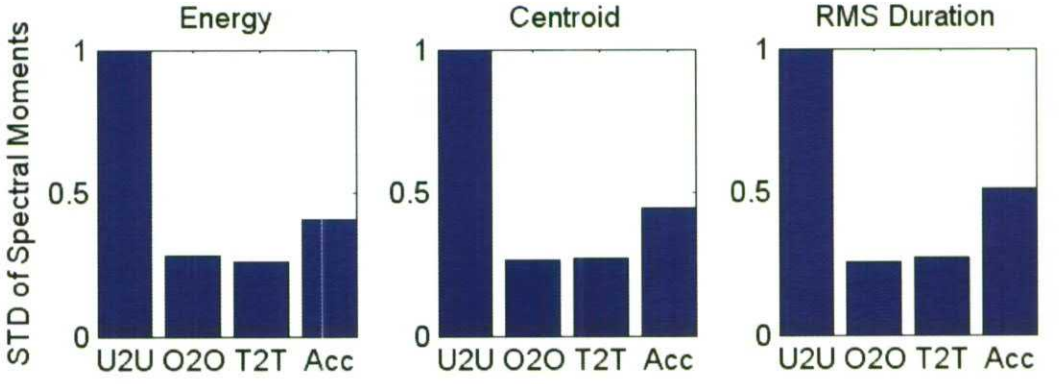

Figure 9: Normalized standard deviation of spectral moments for FRF21

Principal Component Analysis

The next feature we examined was the principal components of the impulse and frequency-response functions from Channel 2. Given N samples of data in p dimensions, $(x_1, x_2, \ldots, x_p)$, principal component analysis (PCA) seeks to project the data into a new p-dimensional set of Cartesian coordinates $(z_1, z_2, \ldots, z_p)$ by a linear transformation [6]. The goal of PCA is to conduct data reduction in such a way that this linear combination of the original variables contains as much of the total variance as possible when projected into the reduced space.

The principal coordinates are calculated as follows: Given data $\mathbf{x}_i = [x_{1i}, x_{2i}, \ldots, x_{pi}]^{\mathrm{T}}$, where the index i varies from 1 to N, the covariance matrix $\boldsymbol{\Sigma}$ is formed:

$$\boldsymbol{\Sigma} = \sum_{i=1}^{N} (\mathbf{x}_i - \bar{\mathbf{x}})(\mathbf{x}_i - \bar{\mathbf{x}})^{\mathrm{T}} \tag{6}$$

where $\bar{\mathbf{x}}$ denotes the mean vector of the x_i's. Because it is, by definition, symmetric and positive semidefinite, the covariance matrix can then be decomposed into a set of eigenvalues and eigenvectors:

$$\boldsymbol{\Sigma} = \mathbf{V} \boldsymbol{\Lambda} \mathbf{V}^{\mathrm{T}} \tag{7}$$

where $\boldsymbol{\Lambda}$ is a diagonal matrix containing the ranked eigenvalues of $\boldsymbol{\Sigma}$, and $\mathbf{V}$ is the matrix containing the corresponding eigenvectors. Note that the singular value decomposition can be used for this step. The transformation to principal components is then:

$$\mathbf{z}_i = \mathbf{V}^{\mathrm{T}} (\mathbf{x}_i - \bar{\mathbf{x}}) \tag{8}$$

This means that the coordinates $\mathbf{z}_i$ are the projection of the original $\mathbf{x}_i$ onto the eigenvectors defined by the columns of matrix $\mathbf{V}$. These eigenvectors are called the principal components, and the coordinates $\mathbf{z}_i$ are called the *scores*.

There are as many principal components as there are data points, but the first principal component accounts for as much of the variability in the data as possible. Each succeeding component accounts for as much of the remaining variability as possible, and so on. Therefore, only a few principal components are needed to represent the data. The coefficients in the eigenvector matrix that relate the original functions to the principal components are the features of interest here. In other words, the variation of these coefficients is used to assess the variability of the data sets within a test group.

The first principal component of the impulse response at Channel 2 accounts for 26.9% of the variation in the data, while the first nine principal components have a cumulative variance of 86.7%. Visually, there is little significance in the principal components themselves. The principal component coefficients are used to assess the variability in the data within each test group by examining the standard deviation of these coefficients.

Figure 10 shows that the relative variations between the test groups are similar for all but the second principal component, with U_2U variability again being the highest. It is believed that the second principal component might be dominated by the noise in the signal, which would explain the reason that the variability is high for all test groups.

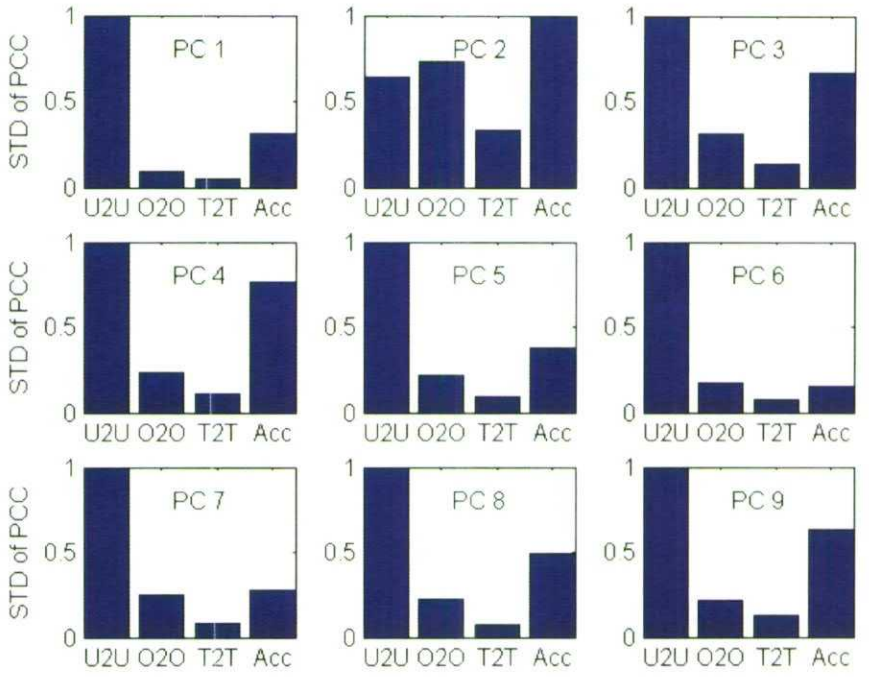

Figure 10: Normalized standard deviation of PCA coefficients for impulse responses at Channel 2.

We repeated the principal component analysis for the frequency response functions from Channel 2. The first component appears to encompass more of the variability in the data (35.9% of the variance) than the first component of the impulse-response data (26.9% of the variance). The first nine principal components capture 80.6% of the variance in the data. The variation between the coefficients within a test group is shown in Figure 11. Note that only the magnitude of the FRF is used to extract the principal components.

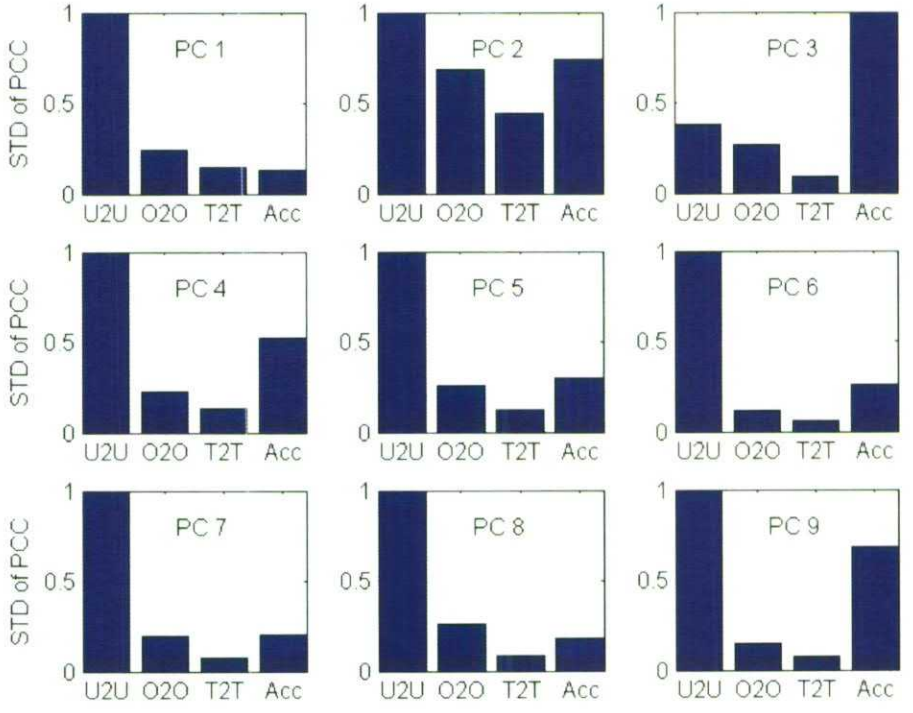

Figure 11: Normalized standard deviation of PCA coefficients for FRF21.

CONCLUSION

The purpose of this report was to examine the sources of variability in a series of modal tests performed on a population of spherical floats. We focused on four areas of variability: the variation between the individual floats (U_2U), the variation caused by using different operators to perform the test (O_2O), the variation in the test setup (T_2T), and the variability caused by placing the accelerometers in slightly different positions on the sphere (Acc).

We used a collection of tools to try to assess the amount of variability caused by each of these sources. From these methods, the following conclusions were drawn: U_2U variability, as expected, is the largest by a significant margin; second largest is (in general) the variability caused by Acc. This variation should be larger than that caused by the T_2T repetition, because the same procedure used in the T_2T measurements is performed to move the accelerometers to different positions. Thus, Acc encompasses two sources of variability. Most methods find this intuition to be true, with O_2O variability contributing about the same as T_2T variability.

The methods we used to assess variability in the data to reach the above conclusions include the following: standard deviation of the IRFs and FRFs, the variation of the frequency values for the first four modes, the temporal and spectral moments, and the principal components of the time response. Small deviations from these conclusions occurred in: the first principal component of the frequency response, which showed the Acc variability to be only slightly less than the T_2T variability; in the first mode, which showed the Acc variability to be slightly lower than T_2T variability; and finally in the fourth mode, which showed Acc to be more significant than the choice of float unit. These exceptions are not significant and lead us to believe that we have made a robust assessment of the major contributors to the variation in the modal-response data.

REFERENCES

1. S. W. Doebling, A. Robertson, R. Dolin, J. Pepin, J. Schultze, T. J. Ross, E. Rodriguez, C. Treml, and N. Shah, "Quantifying and Incorporating Parametric Uncertainty for the Prediction of the Nonlinear Crush Behavior of a Population of Steel Marine Floats," Los Alamos National Laboratory Report LA-MS-13983 (March 2002).
2. J. E. Pepin, B. H. Thacker, E. A. Rodriguez, and D. S. Riha, "A Probabilistic Analysis of a Nonlinear Structure Using Random Fields to Quantify Geometric Shape Uncertainties," in *Proceedings of the 43rd AIAA/ASME/ASCE/ASH Structures, Structural Dynamics, and Materials Conference* (Denver, Colorado, April 22–25, 2002).
3. Quality Float Works, 1382 Payne Road, Schaumburg, IL 60173.
4. J. N. Juang, *Applied System Identification* (Prentice Hall, Englewood Cliffs, New Jersey, 1994).
5. D. O. Smallwood, "Characterizing Transient Vibrations Using Band Limited Moments," in *Proceedings of the 60th Shock and* Vibration *Symposium* (hosted by the David Taylor Research Center, Underwater Explosions Research Division, Portsmouth, Virginia, November 1989) Vol. III, pp. 93–112.
6. W. R. Dillon, M. Goldstein, *Multivariate Analysis: Methods and Applications* (John Wiley & Sons, New York City, New York, 1984).